

Title	ORCHIDEE-PEAT (revision 4596), a model for northern peatland CO <sub>2</sub> , water, and energy fluxes on daily to annual scales
Authors	Qiu, Chunjing;Zhu, Dan;Ciais, Philippe;Guenet, Bertrand;Krinner, Gerhard;Peng, Shushi;Aurela, Mika;Bernhofer, Christian;Bruemmer, Christian;Bret-Harte, Sydonia;Chu, Housen;Chen, Jiquan;Desai, Ankur R.;Dusek, Jiri;Euskirchen, Eugenie S.;Fortuniak, Krzysztof;Flanagan, Lawrence B.;Friborg, Thomas;Grygoruk, Mateusz;Gogo, Sebastien;Gruenwald, Thomas;Hansen, Birger U.;Holl, David;Humphreys, Elyn;Hurkuck, Miriam;Kiely, Gerard;Klatt, Janina;Kutzbach, Lars;Largerón, Chloe;Laggoun-Defarge, Fatima;Lund, Magnus;Lafleur, Peter M.;Li, Xuefei;Mammarella, Ivan;Merbold, Lutz;Nilsson, Mats B.;Olejnik, Janusz;Ottosson-Lofvenius, Mikael;Oechel, Walter;Parmentier, Frans-Jan W.;Peichl, Matthias;Pirk, Norbert;Peltola, Olli;Pawlak, Włodzimierz;Rasse, Daniel;Rinne, Janne;Shaver, Gaius;Schmid, Hans Peter;Sottocornola, Matteo;Steinbrecher, Rainer;Sachs, Torsten;Urbaniak, Marek;Zona, Donatella;Ziemblińska, Klaudia
Publication date	2018
Original Citation	Qiu, C., Zhu, D., Ciais, P., Guenet, B., Krinner, G., Peng, S., Aurela, M., Bernhofer, C., Brümmer, C., Bret-Harte, S., Chu, H., Chen, J., Desai, A. R., Dušek, J., Euskirchen, E. S., Fortuniak, K., Flanagan, L. B., Friborg, T., Grygoruk, M., Gogo, S., Grünwald, T., Hansen, B. U., Holl, D., Humphreys, E., Hurkuck, M., Kiely, G., Klatt, J., Kutzbach, L., Largerón, C., Laggoun-Défarge, F., Lund, M., Lafleur, P. M., Li, X., Mammarella, I., Merbold, L., Nilsson, M. B., Olejnik, J., Ottosson-Löfvenius, M., Oechel, W., Parmentier, F. J. W., Peichl, M., Pirk, N., Peltola, O., Pawlak, W., Rasse, D., Rinne, J., Shaver, G., Schmid, H. P., Sottocornola, M., Steinbrecher, R., Sachs, T., Urbaniak, M., Zona, D. and Ziemblińska, K. (2018) 'ORCHIDEE-PEAT (revision 4596), a model for northern peatland CO <sub>2</sub> , water, and energy fluxes on daily to annual scales', Geoscientific Model Development, 11(2), pp. 497-519. doi:10.5194/gmd-11-497-2018
Type of publication	Article (peer-reviewed)
Link to publisher's version	<a href="https://www.geosci-model-dev.net/11/497/2018/">https://www.geosci-model-dev.net/11/497/2018/</a> - 10.5194/gmd-11-497-2018

Rights	© 2018, the Author(s). This work is distributed under the Creative Commons Attribution 4.0 License. <a href="https://creativecommons.org/licenses/by/4.0/">https://creativecommons.org/licenses/by/4.0/</a> - <a href="https://creativecommons.org/licenses/by/4.0/">https://creativecommons.org/licenses/by/4.0/</a>
Download date	2025-07-31 23:59:27
Item downloaded from	<a href="https://hdl.handle.net/10468/5590">https://hdl.handle.net/10468/5590</a>





*Supplement of*

## **ORCHIDEE-PEAT (revision 4596), a model for northern peatland CO<sub>2</sub>, water, and energy fluxes on daily to annual scales**

**Chunjing Qiu et al.**

*Correspondence to:* Chunjing Qiu ([chunjing.qiu@lsce.ipsl.fr](mailto:chunjing.qiu@lsce.ipsl.fr))

The copyright of individual parts of the supplement might differ from the CC BY 4.0 License.

## Supplement

### Text S1

Temperature and moisture functions are used to parameterize the decrease of soil carbon decomposition under cold, and / or dry (or too wet) soil conditions (Krinner et al., 2005), given by:

Temperature inhibition function:

$$F_T = \min \left( 1, \exp \left( \frac{\ln(Q_{10}) (T - T_{\text{ref}})}{10^\circ\text{C}} \right) \right) ; \text{ with } Q_{10} = 2, T_{\text{ref}} = 30^\circ\text{C} \quad (\text{S1})$$

Moisture inhibition function:

$$F_H = \max(0.25, \min(1.0, aH^2 + bH + c)) ; \text{ with } a=-1.1, b=2.4, c=-0.29 \quad (\text{S2})$$

Temperature (T) and moisture (H) used in equation S1 or S2 are calculated as eleven soil layers-weighted average temperature and moisture respectively as follows:

$$X = \sum_{i=1}^{11} (X_i * r * (\exp(-z_{i-1}/z_{\text{decomp}}) - \exp(-z_i/z_{\text{decomp}}))) \quad (\text{S3})$$

where X is temperature (T) or moisture (H) used in equation S1/ equation S2;  $X_i$  is the temperature ( $T_i$ ) or moisture ( $H_i$ ) of the  $i^{\text{th}}$  soil layer;  $z_i$  is the depth of the node  $i$  (Figure 1);  $z_{\text{decomp}}$  is a scaling depth which parameterized an exponential profile of the decomposers,  $z_{\text{decomp}} = 0.2\text{m}$ ;  $r$  is a scaling factor, given by:

$$r = 1 / (1 - \exp(-z_{11}/z_{\text{decomp}})) ; \text{ with } z_{11} \text{ is the depth of the } 11^{\text{th}} \text{ node, } z_{11} = 2\text{m}$$

In equation S3,  $H_i$  is the relative water content of the  $i^{\text{th}}$  soil layer defined as:

$$H_i = \frac{(\theta_i - \theta_w)}{(\theta_f - \theta_w)} \quad (\text{S4})$$

where  $\theta_i$  is the water content of the  $i^{\text{th}}$  layer,  $\theta_f$  ( $\text{m}^3 \text{ m}^{-3}$ ) is water content at field capacity,  $\theta_w$  ( $\text{m}^3 \text{ m}^{-3}$ ) is water content at permanent wilting point.  $\theta_f = 0.32 \text{ m}^3 \text{ m}^{-3}$ ,  $\theta_w = \theta_r$  (Table 1).

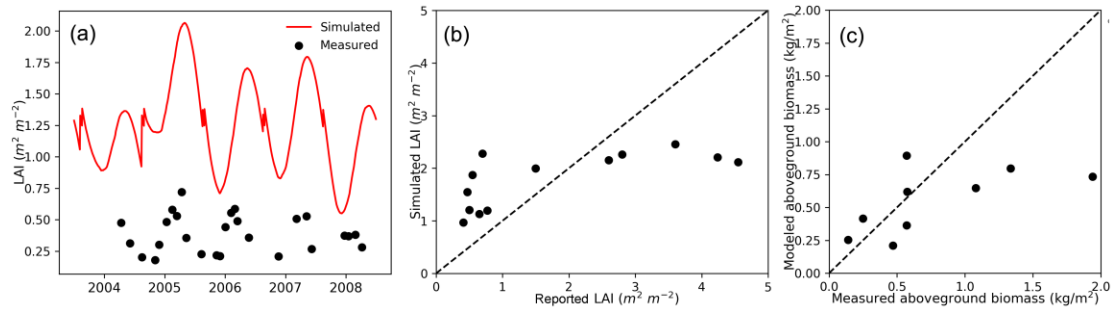


**Fig. S1.** (a) Simulated vs. measured leaf area index (LAI) at the blanket bog IE-Kil, Ireland. (b) Simulated vs. reported (measured/estimated) LAI across peatland sites, dashed line is a hypothetical 1:1 regression line. Note that in (b), the reported LAI was estimated (by eye or from NDVI) at some sites. (c) Simulated vs. measured aboveground biomass, assuming that the carbon content of dry biomass is 50%.

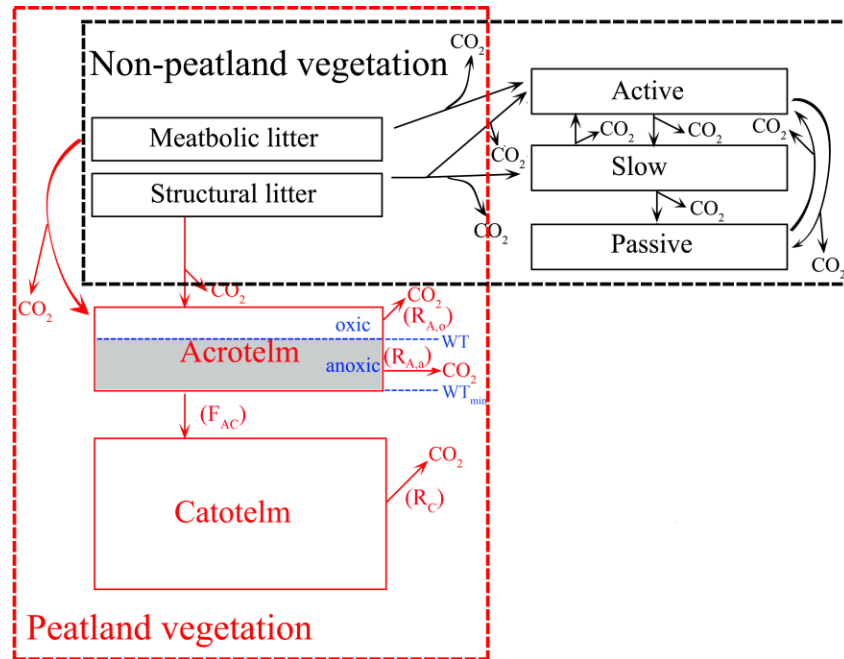


**Fig. S2.** Schematic overview of litter and soil carbon dynamics in ORCHIDEE-PEAT. For non-peatland vegetation (the black dashed box), decompositions of carbon in the two litter pools and three soil pools, and carbon flows between them are adapted from the CENTURY model (Parton et al., 1988); for peatland vegetation (the red dashed box), the active, slow and passive soil carbon pools are replaced by a two-layered model, following Kleinen et al. (2012).

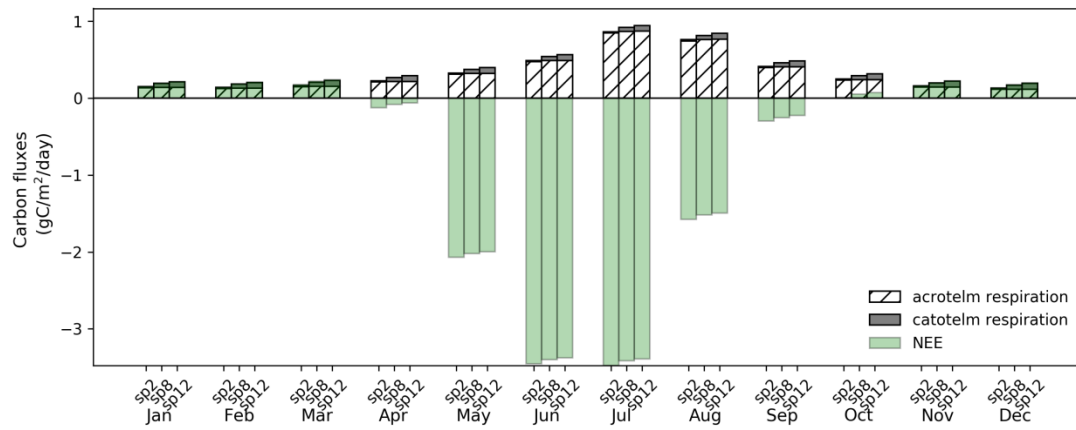


**Fig. S3.** Monthly means of acrotelm and catotelm soil carbon pool respiration, as well as NEE fluxes at CA-Wp1 site (2003 – 2009 mean values). Sp2, sp8, sp12 denotes spin-ups of the model for 2000, 8000 and 12,000 years respectively.

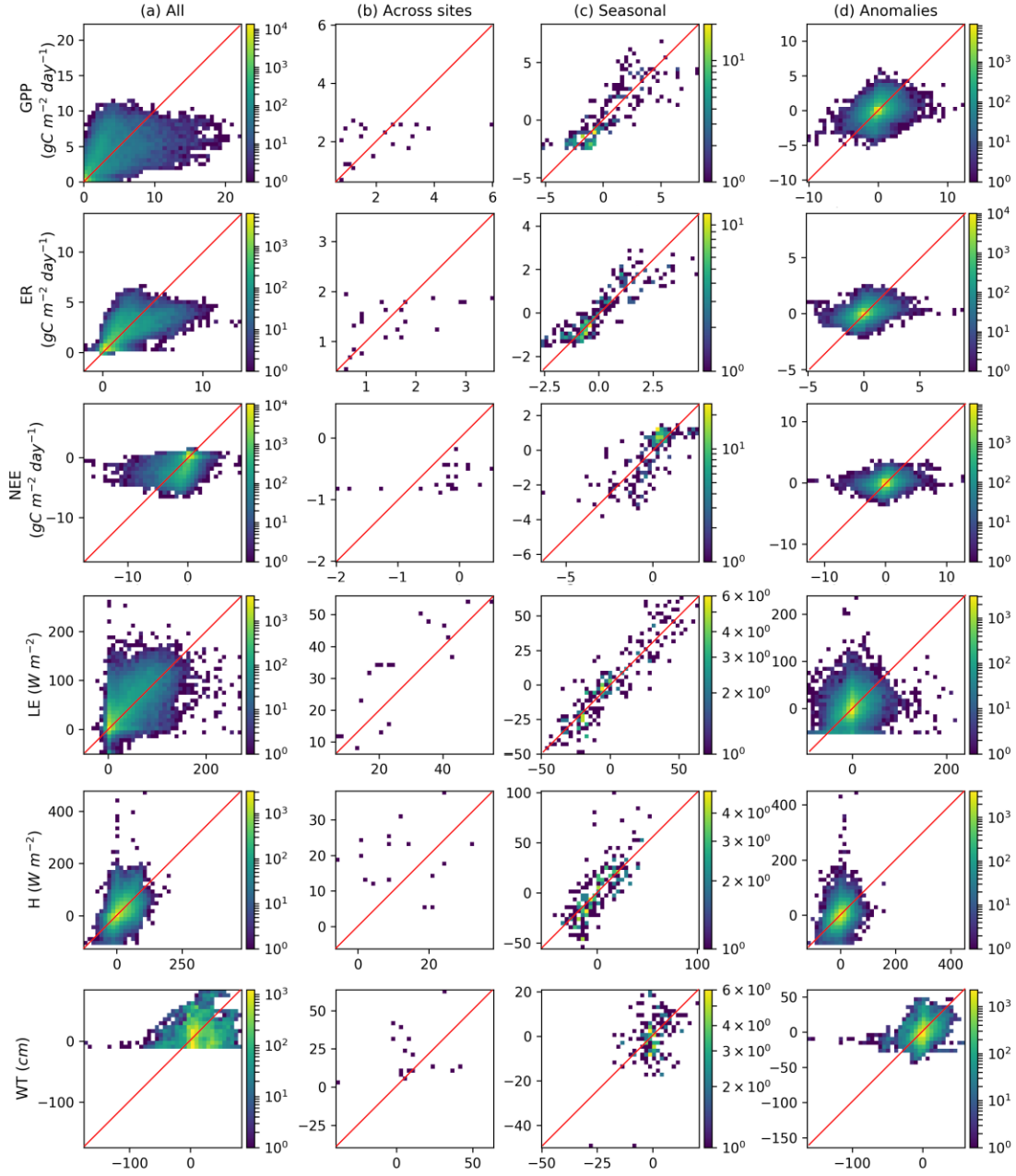


**Fig. S4.** Observed (x-axis) versus simulated (y-axis) fluxes (GPP, ER, NEE, WT, LE, H) at the 22 sites where GPP derived from direct EC measurements were available. Fluxes were simulated using fixed  $V_{\text{cmax}}$  ( $40 \mu\text{mol m}^{-2} \text{s}^{-1}$ ) for peatland vegetation at each site. The colors of points indicate the number of data in each bin, in panel (b) each data point represents one peatland site. The red line identifies the observations = the simulations.



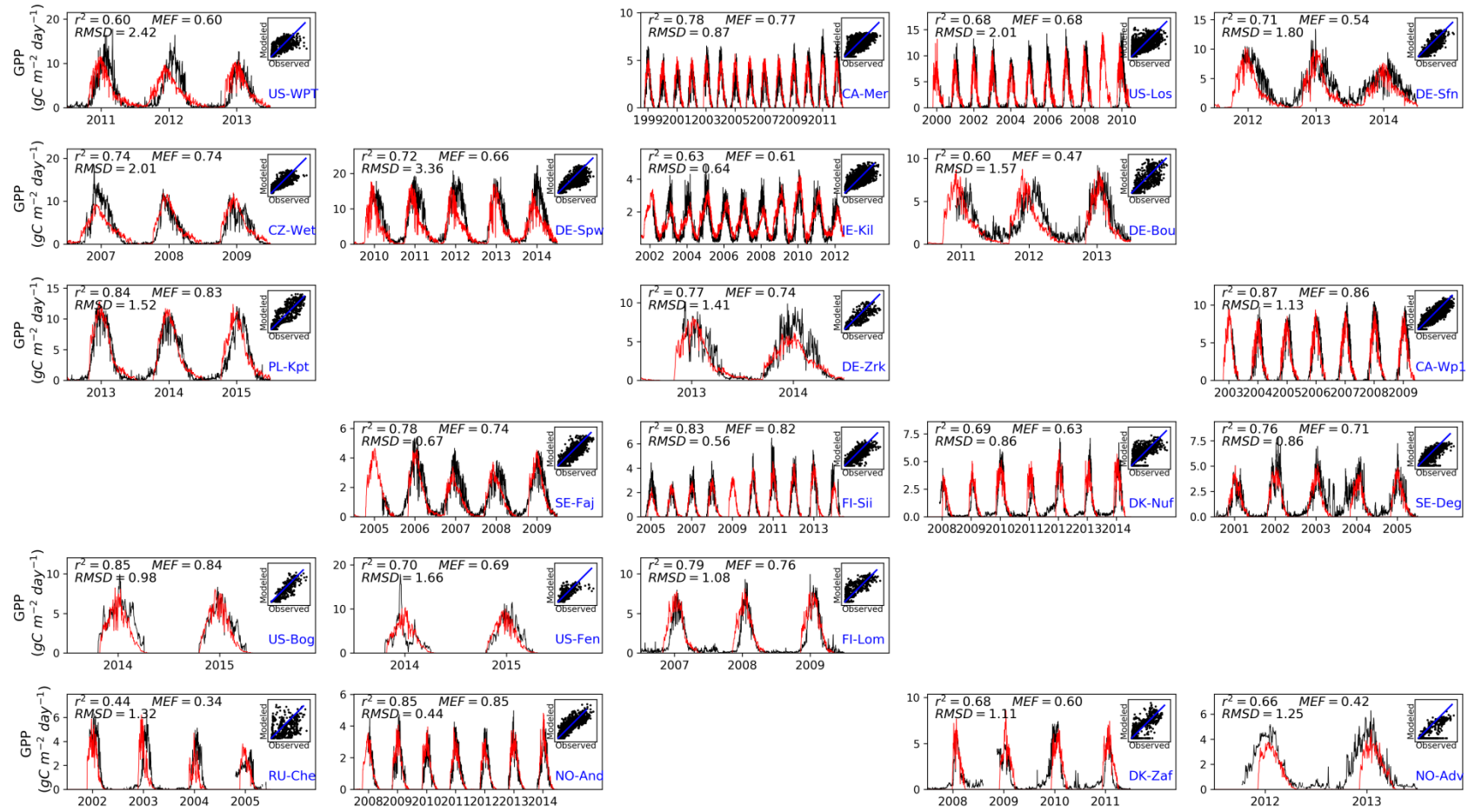


**Fig. S5.** Site-by-site model performance on GPP at a daily time step. Black line: observed GPP; red line: simulated GPP. In the insert, x-axis is observations, y-axis is simulations, the blue line is a hypothetical 1:1 regression line.

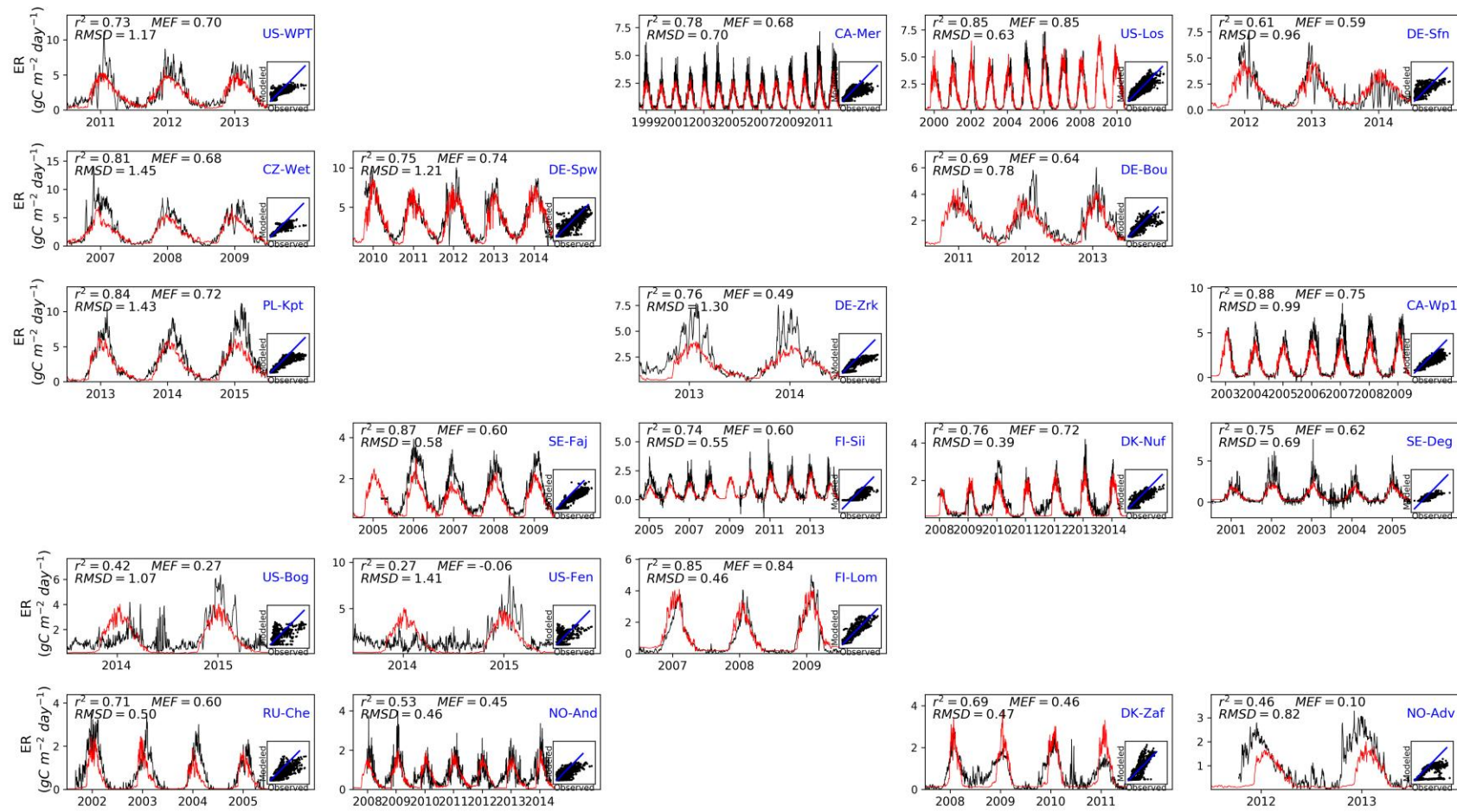


**Fig. S6.** Site-by-site model performance on ER at a daily time step. Black line: observed ER; red line: simulated ER. In the insert, x-axis is observations, y-axis is simulations, the blue line is a hypothetical 1:1 regression line.

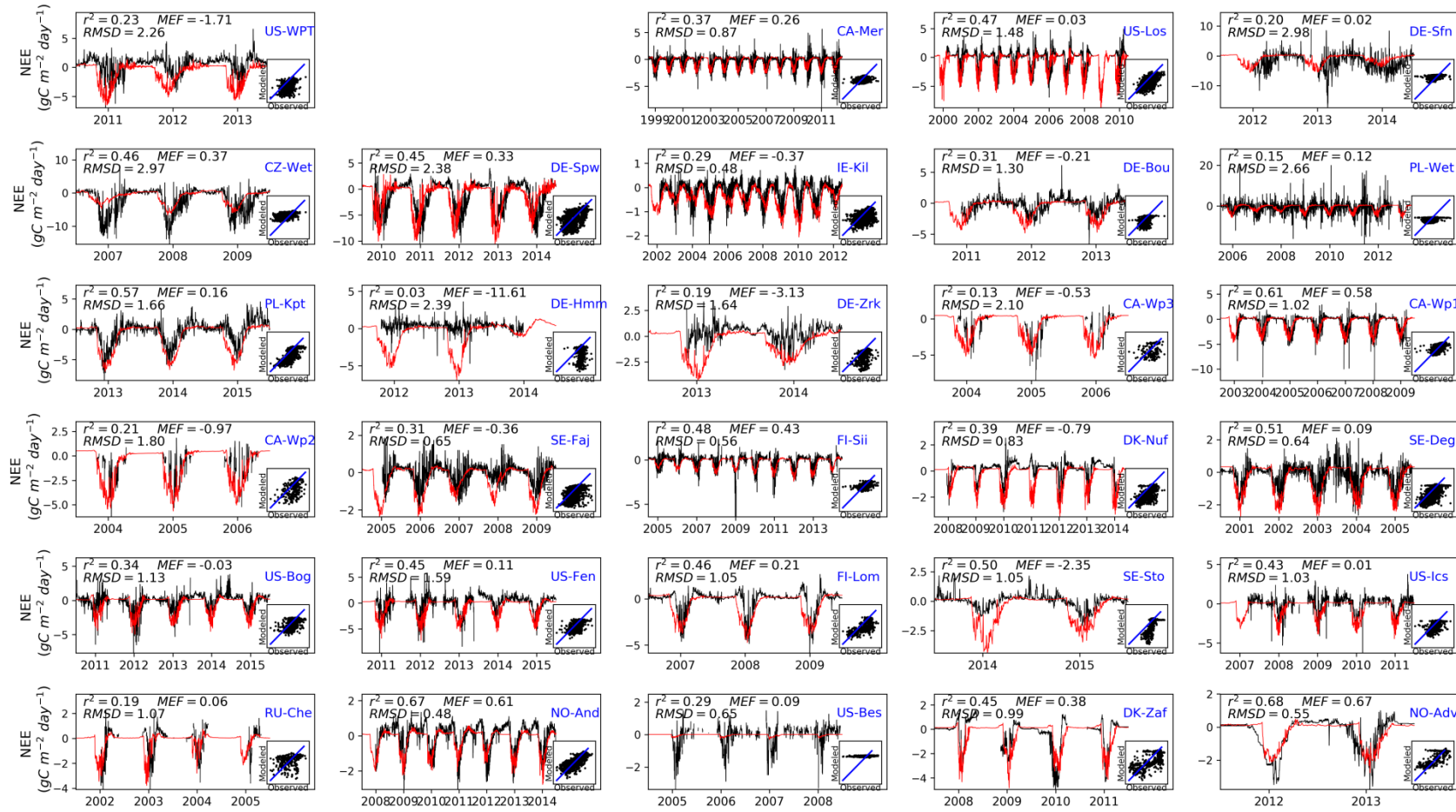


**Fig. S7.** Site-by-site model performance on NEE at a daily time step. For sites where no GPP observations were available to tune  $V_{\text{cmax}}$ , its value was calculated according to relationship between  $V_{\text{cmax}}$  and latitude. Black line: observed NEE; red line: simulated NEE. In the insert, x-axis is observations, y-axis is simulations, the blue line is a hypothetical 1:1 regression line.

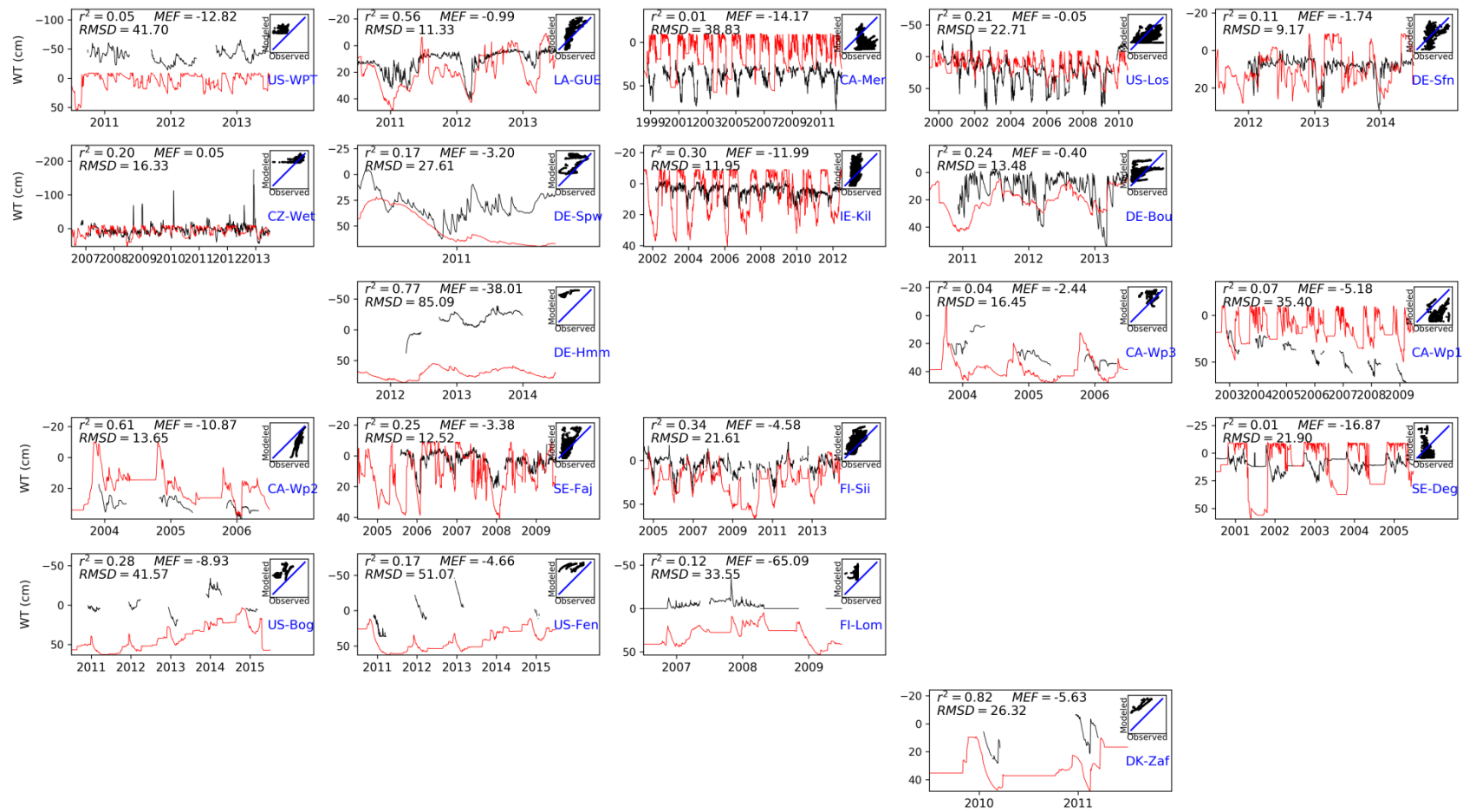


**Fig. S8.** Site-by-site model performance on WT at a daily time step. For sites where no GPP observations were available to tune  $V_{\text{cmax}}$ , its value was calculated according to relationship between  $V_{\text{cmax}}$  and latitude. Black line: observed WT; red line: simulated WT. In the insert, x-axis is observations, y-axis is simulations, the blue line is a hypothetical 1:1 regression line.



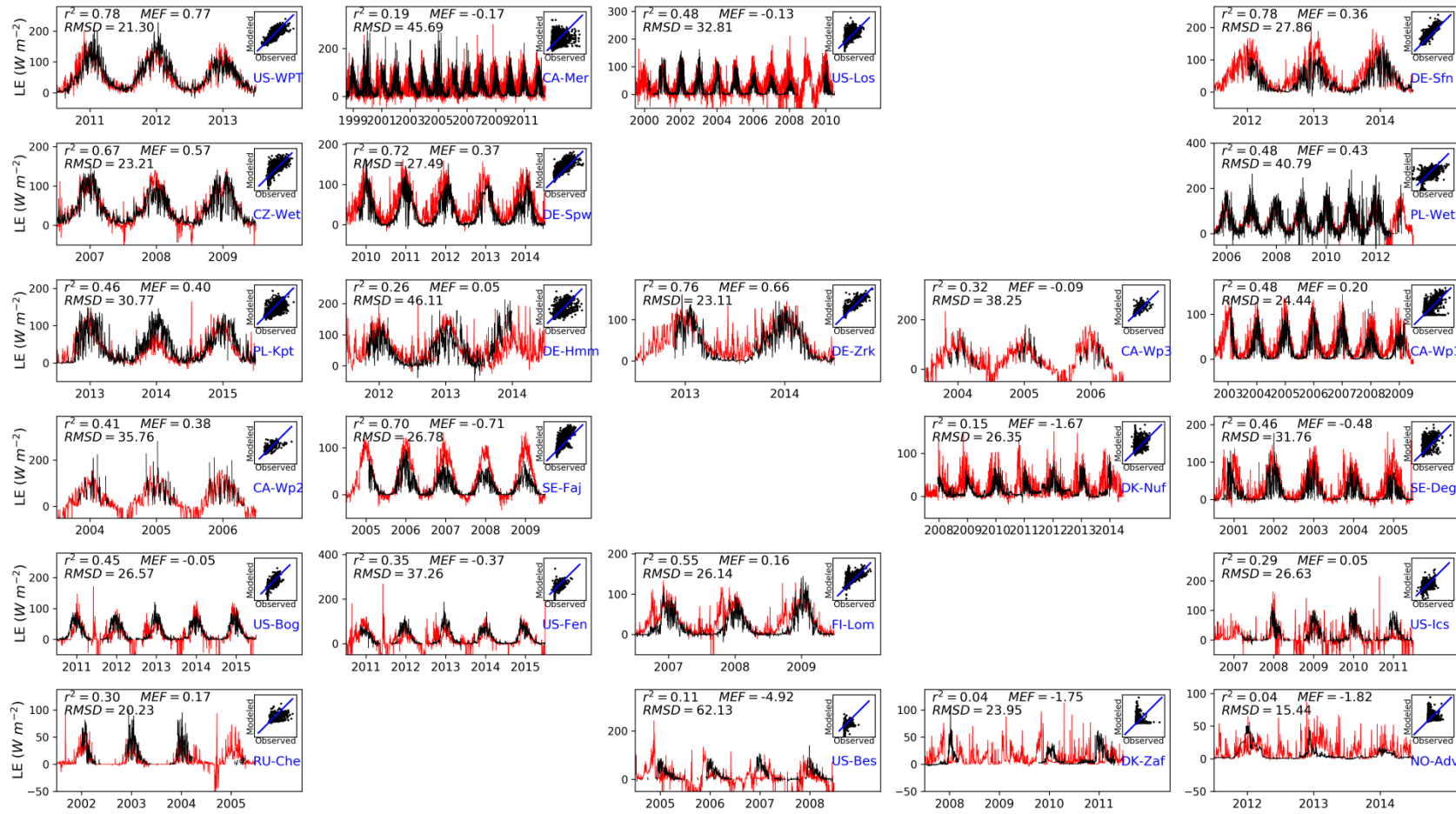


**Fig. S9.** Site-by-site model performance on LE at a daily time step. For sites where no GPP observations were available to tune  $V_{\text{cmax}}$ , its value was calculated according to relationship between  $V_{\text{cmax}}$  and latitude. Black line: observed LE; red line: simulated LE. In the insert, x-axis is observations, y-axis is simulations, the blue line is a hypothetical 1:1 regression line.

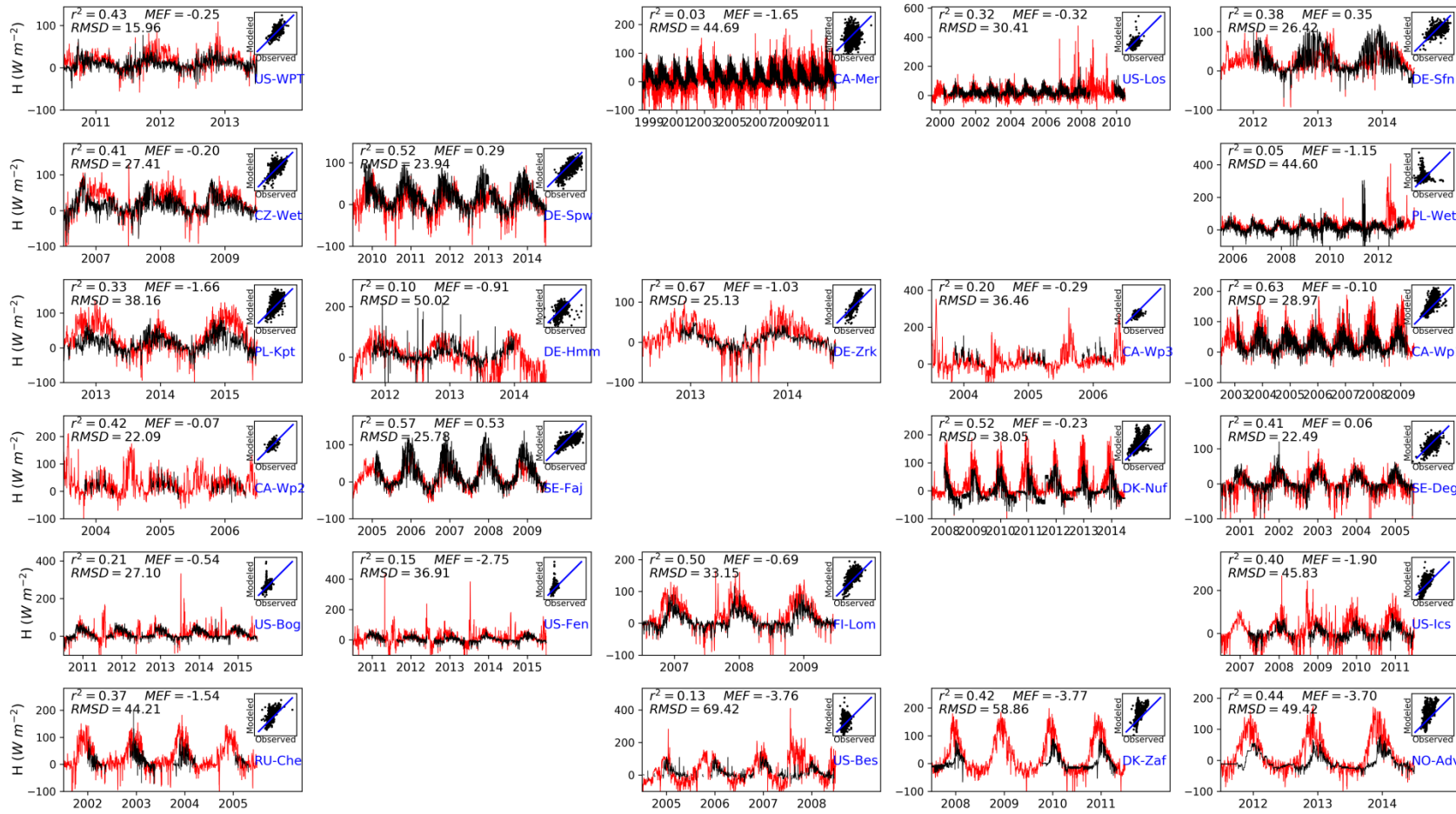


**Fig. S10.** Site-by-site model performance on  $H$  at a daily time step. For sites where no GPP observations were available to tune  $V_{\text{cmax}}$ , its value was calculated according to relationship between  $V_{\text{cmax}}$  and latitude. Black line: observed  $H$ ; red line: simulated  $H$ . In the insert, x-axis is observations, y-axis is simulations, the blue line is a hypothetical 1:1 regression line.

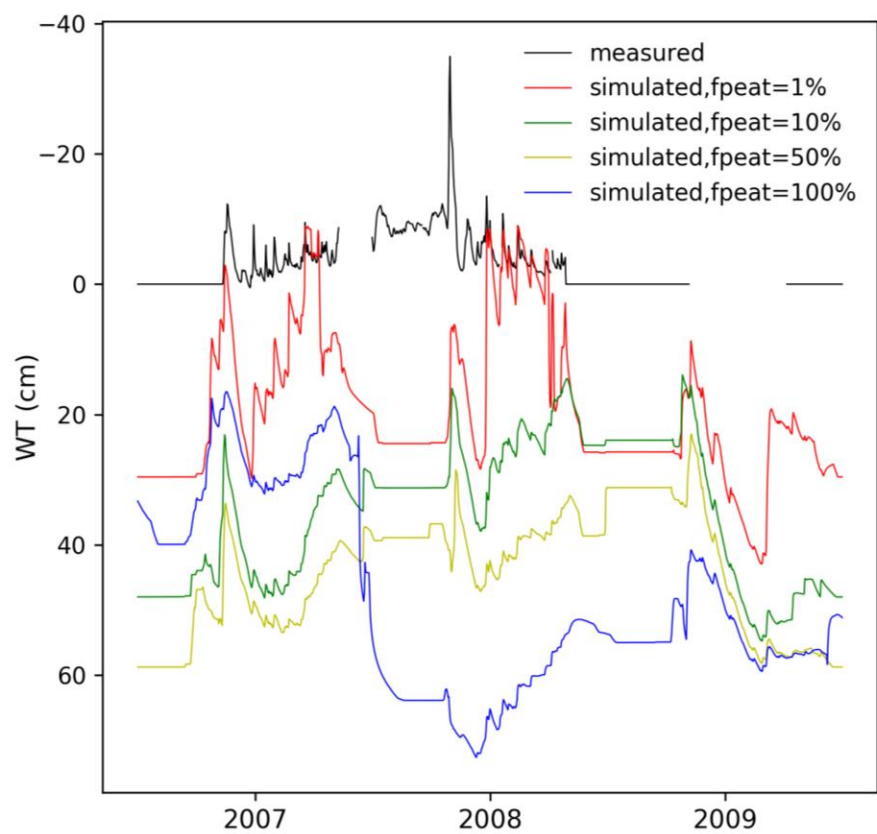


**Fig. S11.** Sensitivity test of simulated water table to peatland area fraction in the grid cell, performed at the fen site FI-Lom.

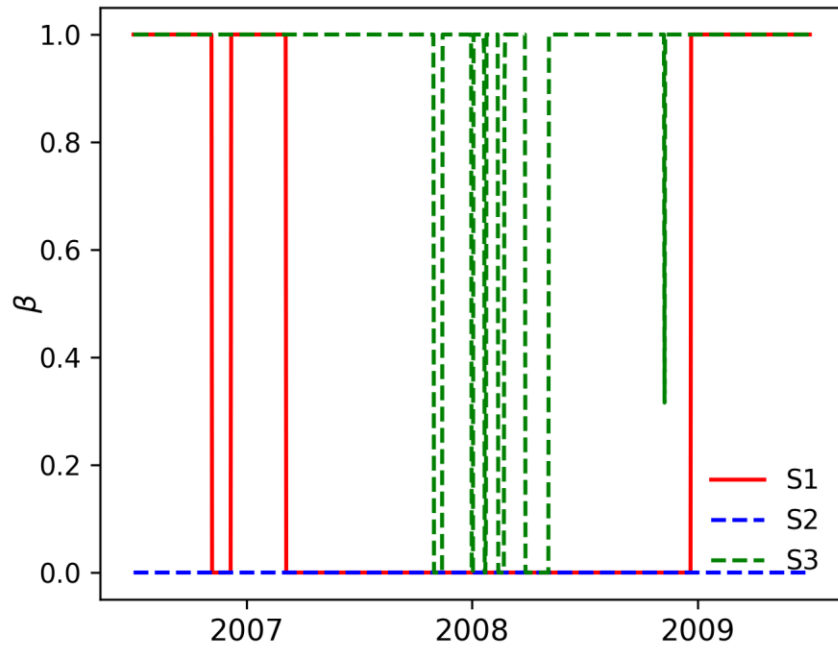


**Fig. S12.** The fraction of the acrotelm where carbon decomposes under oxic conditions ( $\beta$ ) at Lompolojännkä fen site (FI-Lom). S1: simulated water table (WT) were used in the carbon module; S2: observed water table ( $WT_{obs}$ ) were used in the carbon module; S3: assumed that water table were 20cm deeper than simulated results, thus ( $WT-20cm$ ) were used in the carbon module.



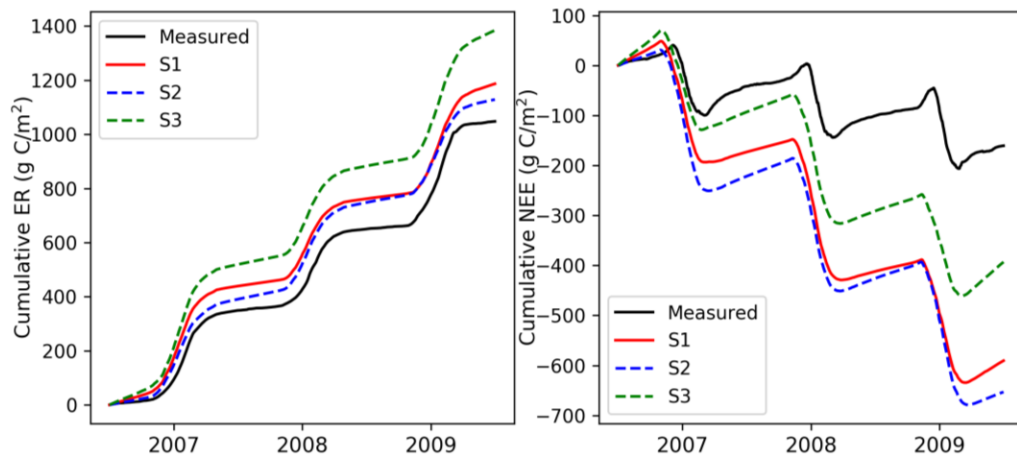


**Fig. S13.** Cumulative ER (left figure) and NEE (right figure) at Lompolojänkämä fen site (FI-Lom). S1: simulated water table (WT) were used in the carbon module; S2: observed water table ( $WT_{obs}$ ) were used in the carbon module; S3: assumed that water table were 20cm deeper than simulated results, thus ( $WT-20cm$ ) were used in the carbon module.

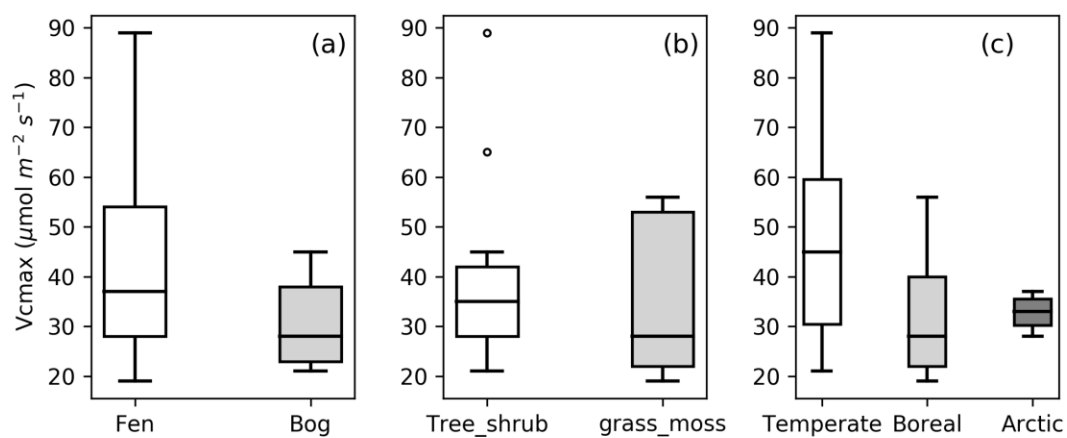


**Fig. S14.** Boxplot of optimized  $V_{cmax}$  for the (a) fen sites and bog sites, (b) tree and/or shrub dominated sites and grass and/or moss dominated sites, (c) temperate sties, boreal sites and arctic sites.

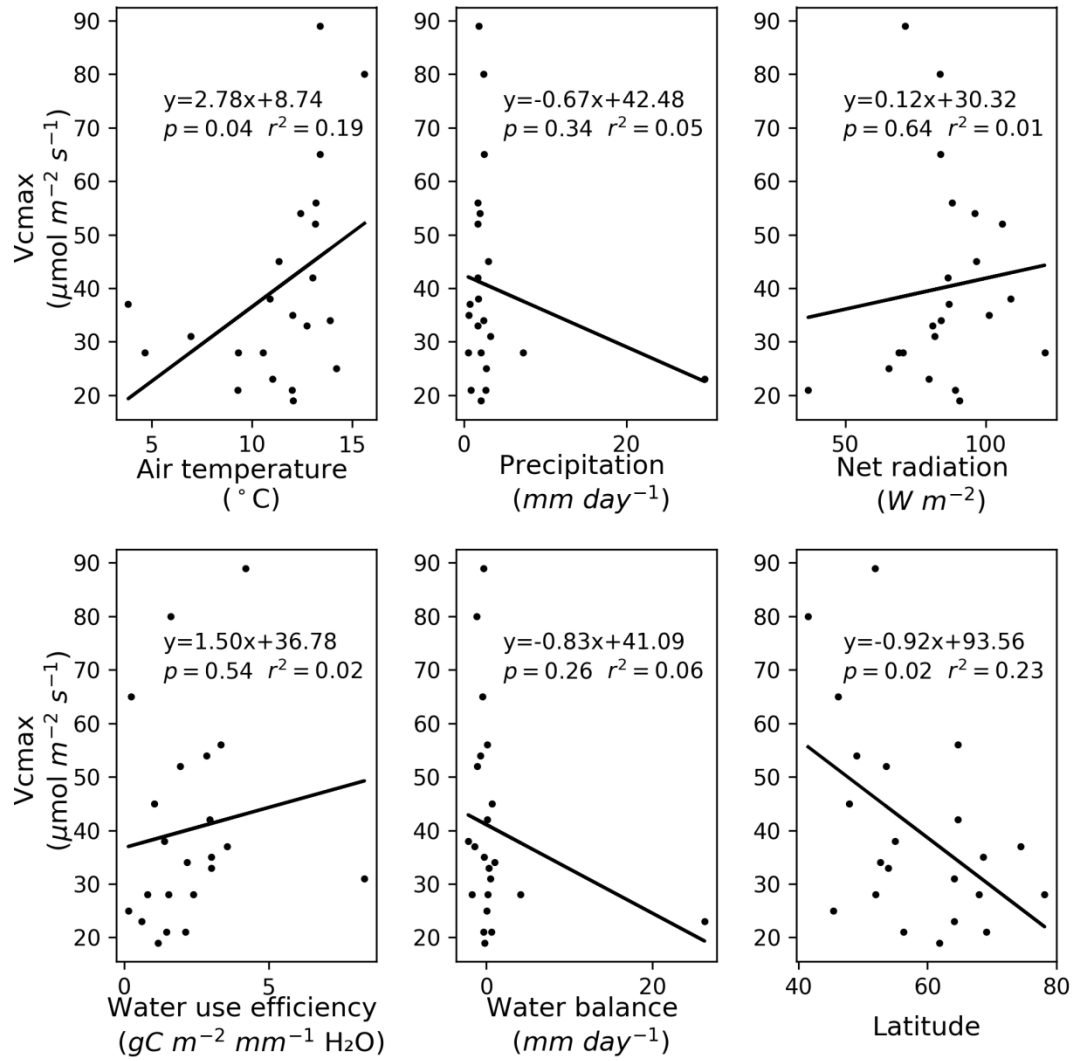


**Fig. S15.** Relationship between optimized  $V_{cmax}$  and meteorological variables and biological parameters, as well as latitude of the sites location.

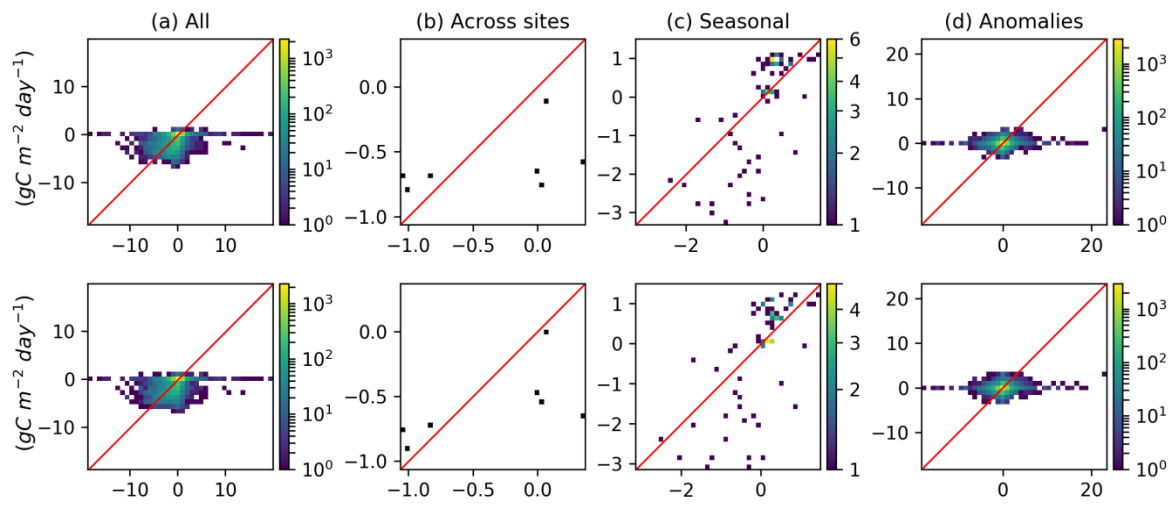


**Fig. S16.** Observed (x-axis) versus simulated (y-axis) NEE at the 7 sites where there were no available observed GPP (derived from direct EC measurements). The upper four plots presented results of the model using mean  $V_{\text{cmax}}$  value ( $40 \mu\text{mol m}^{-2} \text{s}^{-1}$ ), the lower four plots showed results of the same simulation but using  $V_{\text{cmax}}$  values calculated from the empirical relationship between  $V_{\text{cmax}}$  and the latitude of chosen sites location. The colors of points indicate the number of data in each bin, in panel (b) each data point represents one peatland site. The red line identifies the observations = the simulations.

**Table S1.** Number of days with available water table (WT) measurements (the first column), days with WT above the soil surface (the second column,  $WT \leq 0\text{cm}$ ), days with WT remains below 10cm above the soil surface (the third column,  $-10 \leq WT \leq 0$ ) at each site, and the ratio between the third and second column.

site	Measured days	$WT \leq 0$	$-10 \leq WT \leq 0$	Ratio
FI-Sii	3073	907	837	92.28
LA-GUE	1095	0	0	
US-Fen	325	139	58	41.73
US-Bog	552	185	49	26.49
CA-Mer	3699	0	0	
CZ-Wet	2381	854	600	70.26
DE-Bou	937	28	28	100.00
DE-Hmm	545	461	84	18.22
DE-Sfn	914	5	5	100.00
DE-spw	365	14	14	100.00
DK-Zaf	145	29	29	100.00
FI-Lom	886	882	825	93.54
IE-Kil	3772	170	170	100.00
SE-Deg	1825	38	38	100.00
SE-Faj	1285	376	376	100.00
US-Los	3643	383	129	33.68
US-WPT	759	759	0	0.00
CA-Wp1	1075	0	0	
CA-Wp2	514	0	0	
CA-Wp3	531	0	0	
ALL	28321	5230	3242	61.99

**Table S2.** Percent of gaps in measured water table (WT) data at sites used in the second set of simulation (S2).

site	percent of gaps(%)
CZ-Wet	7.43
DE-Sfn	16.53
DE-Bou	14.45
FI-Lom	19.57
IE-Kil	6.05
SE-Deg	0.058
SE-Faj	30.51
US-Los	9.79

## **Sites description**

### **Winous Point North Marsh (US-WPT)**

The marsh is located in the Winous Point Marsh Conservancy along the shore of Lake Erie, dominated by floating-leaved and emergent vegetation. The marsh is relatively isolated by the surrounding dikes but receives runoff from nearby croplands through three free-flowing ditches. The outflow of the marsh is managed to maintain inundation all year round (Chu et al., 2014, 2015).

### **Mer Bleue Eastern Peatland (CA-Mer)**

The Mer Bleue peatland is an undisturbed bog located in east of Ottawa, Canada, dominated by evergreen and deciduous shrubs and *Sphagnum* mosses (Lafleur et al., 2005).

### **Lost Creek shrub fen (US-Los)**

The Lost Creek site is a fen in North Central Wisconsin, USA, dominated by shrubs and sedges. The removal of beaver dams from this site in fall 2000 and summer 2003 partly explains a large decline of the water table in subsequent years (Sulman et al., 2009).

### **Schechenfilz Nord (DE-Sfn)**

Schechenfilz is an undisturbed bog site located in the pre-alpine region of southern Germany, dominated by slow growing bog-pines, peat mosses, heather, bog-bilberry and sedges (Hommeltenberg et al., 2014).

### **CZWET (CZ-Wet)**

This fen site is located in the inundation area of a large human-made lake, Třeboň, Czech Republic, dominated by sedges and grasses. Water level is controlled by a system of ditches and is maintained near the soil surface throughout the year (water level can reach up to 2 m above the ground surface due to flood events caused by snow melting or summer rains storms). As a result of nutrient runoff from the upstream, the site has become gradually eutrophicated since the 1980s (Dušek et al., 2009).

### **Spreewald (DE-Spw)**

The Spreewald site is a forested fen in North-East Germany. Main species of the deciduous forest are alder (*Alnus glutinosa*) and ash (*Fraxinus excelsior*) among others (oak, elm, black

cherry). Despite the low precipitation the ecosystem is not limited by water availability due to lateral water flow of the Spree river.

#### **Killorglin - Glencar (IE-Kil)**

This is an undisturbed Atlantic blanket bog located near Glencar, Ireland. Grasses, sedges and shrubs covering together about 30% of the peatland while mosses' cover is about 25% (McVeigh et al., 2014; Sottocornola et al., 2009).

#### **Bourtanger Moor (DE-Bou)**

The Bourtanger Moor site is a semi-natural bog located in a natural park in Northwest Germany and Northeast Netherlands. The study area is a protected but moderately drained bog, dominated by bog heather, purple moor grass, cotton grass, coppices and *Sphagnum* mosses. The site is surrounded by intensive agricultural land use and is thus exposed to elevated atmospheric N deposition of about 25 kg N ha<sup>-1</sup> yr<sup>-1</sup> (Hurkuck et al., 2016).

#### **Rzecin wetland (PL-Wet)**

The Rzecin site is an undisturbed fen located in the north-west Poland, dominated by *Sphagnum* mosses, sedges, and shrubs (Chojnicki et al., 2007). The peatland is a result of the shallowing of the lake, which is much diminished but still exists. According with old maps from the 18th and 19th centuries, in the southern part of the peatland was a natural spring. It was joined to a drainage ditch in the second half of the 19th century (Barabach, 2012). The peatland is surrounded by a relatively tight ring of pastures and cultivated fields and pine forest outside of it. Since 2006, Rzecin peatland has been one of the sites of the Nature 2000 network in Europe (PLH300019) because of its unique flora and plant communities, biodiversity, and presence of relics and rare species (Milecka et al., 2016)

#### **Kopytkowo (PL-Kpt)**

Kopytkowo is a nearly undisturbed fen located in the Middle Basin of the Biebrza Valley, near to the village Kopytkowo, Poland. The measurement site is located close to the Kopytkówka river. The dominant vegetation is high sedges, reed and ferns (Fortuniak et al., 2017).

#### **Himmelmoor (DE-Hmm)**



Himmelmoor is a degraded bog located northwest of Hamburg. Since the 18th century, peat in the area has been drained and cut, with peat mining being stopped only in 2016. Parts of the bog are rewetted with drainage blocking and cutting birch trees since 1980s. The measurement was taken in the area between the newly rewetted part and the still drained part. This area is mainly bare peat with a small fraction of vegetated area (~10%), namely *Betula pubescens*, *Typha latifolia*, *Salix* spp., *Molinia caerulea*, *Calamagrostis pseudophragmites*, *Eriophorum angustifolium* and *vaginatum* (Vanselow-Algan et al., 2015).

#### **Polder Zarnekow (DE-Zrk)**

The Polder Zarnekow fen is located in the Peene river valley, Pomerania, Germany. The site was drained since the 18th century and rewetting began in winter 2004/2005. Surface of this area consist of two main types: open water which is vegetated with submerged and floating vegetation, and emergent grasses (Franz et al., 2016).

#### **Western Peatland (CA-Wp1)**

This is an undisturbed moderately rich fen, located in Alberta, dominated by stunted trees, tall shrubs, and mosses. It is a moderately 'rich' treed fen—rich in species richness, not nutrient availability (Flanagan and Syed, 2011).

#### **Western Peatland poor fen (CA-Wp2), Western Peatland Rich Fen (CA-Wp3)**

These two sites are undisturbed fens located in north Central Alberta, about 150km apart and experienced similar variations in weather. Surface water of the poor fen is more acidic and has poorer nutrient than surface water of the extreme-rich fen. The poor fen (CA-Wp2) is dominated by *Sphagnum* mosses, dwarf evergreen shrubs and trees, sedges and herbs. The extreme-rich fen (CA-Wp3) is dominated by sedges, mosses (Adkinson et al., 2011).

#### **Fåjemyr (SE-Faj)**

The Fåjemyr site is an undisturbed bog located in southern Sweden, dominated by dwarf shrubs, sedges and *Sphagnum* mosses. The N deposition at the study site is 15-20 kg N ha<sup>-1</sup> yr<sup>-1</sup> (Lund et al., 2007, 2012).

#### **Siikaneva fen (FI-Sii)**

Siikaneva site is located at the 12 km<sup>2</sup> Siikaneva wetland complex, containing both minerotrophic (fen) and ombrotrophic (bog) surfaces. Siikaneva is located in southern Finland, the Siikaneva fen site is on a fen surface and is an undisturbed nutrient-poor fen dominated by sedges and a *Sphagnum* carpet. The site is surrounded by Scots pine forest and has a relatively flat microtopography (Aurela et al., 2007; Riutta et al., 2007) .

#### **Nuuk Fen (DK-NuF)**

The undisturbed fen is located in the low-Arctic Kobbefjord valley in southwest Greenland, ca. 20 km from the Greenland capital of Nuuk, dominated by various sedges (Westergaard-Nielsen et al., 2013).

#### **Degerö Stormyr (SE-Deg)**

The Degerö Stormyr is an undisturbed fen located in the Kulb äksliden Experimental Forests, Sweden, dominated by shrubs, sedges, as well as mosses. It is composed of interconnected smaller mires, divided by islets and ridges of glacial till (Nilsson et al., 2008; Sagerfors et al., 2008).

#### **Alaska Bog (US-Bog), Alaska Fen (US-Fen)**

These two sites are located in the boreal peatland lowlands of the Tanana Flats of interior Alaska. They were about 0.5 km apart. US-bog is a collapse scar ombrotrophic bog, with active thaw margins, significant dieback of black spruce trees (*Picea mariana*) and *Sphagnum* moss. The bog is a circular depression that formed through thermokarst.

US-fen is an undisturbed fen, it lacks near-surface permafrost and is dominated by grasses, sedges and forbs (Euskirchen et al., 2014).

#### **Lompoloj änkä (FI-Lom)**

The Lompoloj änkä nutrient rich fen is located in the aapa mire region of north-western Finland, dominated by *Menyanthes trifoliata*, *Salix lapponum* and *Carex* spp and mosses. There is a small stream flows through the site (Aurela et al., 2009).

#### **Abisko Stordalen Palsa Bog (SE-Sto)**

The undisturbed bog is located in the Stordalen peatland complex, northern Sweden, dominated by dwarf shrubs, mosses, lichens and sedges. The discontinuous permafrost in the area is currently thawing (Malmer et al., 2005; Olefeldt et al., 2012).

#### **Imnavait Creek Watershed wet sedge tundra (US-Ics)**

This fen is situated in the northern foothills of the Brooks Range, Alaska, dominated by sedges and dwarf shrubs. There is continuous permafrost underlying this area (Euskirchen et al., 2012, 2016).

#### **Cherski (RU-Che)**

The tundra is located in a flood-plain of the Kolyma river in Northeast Siberia, it is flooded periodically in spring, and dominated by sedges, cotton grass, marsh cinquefoil and few dwarf shrubs. Thawing of the active layer of permafrost and flood water maintained a stagnant water table below the grass canopy (Corradi et al., 2005). The site was drained in fall 2004 and continuous to be drained to study drainage effects on carbon fluxes (Merbold et al., 2009).

#### **Andøya (NO-And)**

Andøya is an undisturbed blanket bog on the island of Andøya, Northern Norway. Dominant vegetation types are mosses, lichens and shrubs. Seasonal temperature variations are attenuated by the maritime influence of the nearby Atlantic Ocean, there is no permafrost at this site due to this maritime settings (Lund et al., 2015).

#### **Barrow-Bes (US-Bes)**

The tundra is located in the large-scale manipulation experiment area in the Alaskan Arctic at the Barrow Environmental Observatory (BEO). The area is underlain by continuous permafrost, dominant vegetations are mosses, sedges and grasses. US-Bes in this study is the south tower (control site) in the manipulation experiment performed from 2007-2009 (Zona et al., 2009).

#### **Zackenberg Fen (DK-Zaf)**

The undisturbed fen is located in the high-Arctic Zackenberg valley, Northeast Greenland National Park. The area is underlain by permafrost and dominated by sedges and mosses (Stiegler et al., 2016).

### **Adventdalen (NO-Adv)**

The Adventdalen site is located on a river terrace on the flat part of a large alluvial fan at the bottom of a glacial valley on Svalbard. The site features continuous permafrost, with typically about 70 cm active layer depth and polygonal ground patterns creating fen conditions. The vegetation is dominated by *Salix polaris* in drier areas, *Eriophorum scheuchzeri* in wetter locations, and moss species in usually inundated spots (Pirk et al., 2016).

### **La Guette**

La Guette peatland is a fen located in Sologne (center part of France, 200 km south of Paris). The site experiences hydrological disturbance caused by a road drain crossing the site at the output which accelerates runoff losses. Work was undertaken in 2014 to restore the hydrological functioning and vegetation of the site (D'Angelo et al., 2016; Laggoun-d et al., 2016). The vegetation is dominated by *Molinia caerulea*, ericaceous shrubs (*Erica tetralix* and *Calluna vulgaris*) and trees (*Pinus sylvestris* and *Betula* spp, mainly on its borders). Mosses (*Sphagnum* spp), *Eriophorum angustifolium* and *Rhyncospora alba* can be dominant in the wettest parts of the site.

### **References**

- Adkinson, A. C., Syed, K. H. and Flanagan, L. B.: Contrasting responses of growing season ecosystem CO<sub>2</sub> exchange to variation in temperature and water table depth in two peatlands in northern Alberta, Canada, , 116, 1–17, doi:10.1029/2010JG001512, 2011.
- Aurela, M., Riutta, T., Laurila, T., TUOVINEN, J., Vesala, T., TUITTILA, E., Rinne, J., Haapanala, S. and Laine, J.: CO<sub>2</sub> exchange of a sedge fen in southern Finland—the impact of a drought period, *Tellus B*, 59(5), 826–837, 2007.
- Aurela, M., Lohila, A., Tuovinen, J. P., Hatakka, J., Riutta, T. and Laurila, T.: Carbon dioxide exchange on a northern boreal fen, *Boreal Environ. Res.*, 14(4), 699–710,

doi:10.1093/treephys/tpn047, 2009.

Barabach, J.: The history of Lake Rzecin and its surroundings drawn on maps as a background to palaeoecological reconstruction, *Limnol. Rev.*, 12(3), 103–114, doi:10.2478/v10194-011-0050-0, 2012.

Barr, A. G., Black, T. A., Hogg, E. H., Kljun, N., Morgenstern, K. and Nesic, Z.: Inter-annual variability in the leaf area index of a boreal aspen-hazelnut forest in relation to net ecosystem production, *Agric. For. Meteorol.*, 126(3–4), 237–255, doi:10.1029/2002JD003011, 2004.

Chojnicki, B. H., Urbaniak, M., Józefczyk, D., Augustin, J. and Olejnik, J.: Measurements of gas and heat fluxes at Rzecin wetland, *Wetl. Monit. Model. Manag.* Taylor Fr. Group, London, 125–131, 2007.

Chu, H., Chen, J., Gottgens, J. F., Ouyang, Z., John, R., Czajkowski, K. and Becker, R.: Net ecosystem methane and carbon dioxide exchanges in a Lake Erie coastal marsh and a nearby cropland, *J. Geophys. Res. Biogeosciences*, 119(5), 722–740, 2014.

Chu, H., Gottgens, J. F., Chen, J., Sun, G., Desai, A. R., Ouyang, Z., Shao, C. and Czajkowski, K.: Climatic variability, hydrologic anomaly, and methane emission can turn productive freshwater marshes into net carbon sources, *Glob. Chang. Biol.*, 21(3), 1165–1181, doi:10.1111/gcb.12760, 2015.

Corradi, C., Kolle, O., Walter, K., Zimov, S. A. and Schulze, E. D.: Carbon dioxide and methane exchange of a north-east Siberian tussock tundra, *Glob. Chang. Biol.*, 11(11), 1910–1925, doi:10.1111/j.1365-2486.2005.01023.x, 2005.

D'Angelo, B., Gogo, S., Laggoun-Défarge, F., Le Moing, F., Jégou, F. and Guimbaud, C.: Soil temperature synchronisation improves representation of diel variability of ecosystem respiration in Sphagnum peatlands, *Agric. For. Meteorol.*, 223(April), 95–102, doi:10.1016/j.agrformet.2016.03.021, 2016.

Dušek, J., Čížková, H., Czerný, R., Taufarová, K., Šmídová, M. and Janouš, D.: Influence of summer flood on the net ecosystem exchange of CO<sub>2</sub> in a temperate sedge-grass marsh, *Agric. For. Meteorol.*, 149(9), 1524–1530, 2009.

Euskirchen, E. S., Bret-Harte, M. S., Scott, G. J., Edgar, C. and Shaver, G. R.: Seasonal patterns

- of carbon dioxide and water fluxes in three representative tundra ecosystems in northern Alaska, *Ecosphere*, 3(1), art4, doi:10.1890/ES11-00202.1, 2012.
- Euskirchen, E. S., Edgar, C. W., Turetsky, M. R., Waldrop, M. P. and Harden, J. W.: Differential response of carbon fluxes to climate in three peatland ecosystems that vary in the presence and stability of permafrost, , 1576–1595, doi:10.1002/2014JG002683. Received, 2014.
- Euskirchen, E. S., Shaver, G. R., Edgar, C. W. and Romanovsky, V. E.: Long-Term Release of Carbon Dioxide from Arctic Tundra Ecosystems in Alaska, *Ecosystems*, doi:10.1007/s10021-016-0085-9, 2016.
- Flanagan, L. B. and Syed, K. H.: Stimulation of both photosynthesis and respiration in response to warmer and drier conditions in a boreal peatland ecosystem, *Glob. Chang. Biol.*, 17(7), 2271–2287, doi:10.1111/j.1365-2486.2010.02378.x, 2011.
- Fortuniak, K., Pawlak, W., Bednorz, L., Grygoruk, M., Siedlecki, M. and Zieliński, M.: Methane and carbon dioxide fluxes of a temperate mire in Central Europe, *Agric. For. Meteorol.*, 232, 306–318, doi:10.1016/j.agrformet.2016.08.023, 2017.
- Franz, D., Koebisch, F., Larmanou, E., Augustin, J. and Sachs, T.: High net CO<sub>2</sub> and CH<sub>4</sub> release at a eutrophic shallow lake on a formerly drained fen, *Biogeosciences*, 13(10), 3051–3070, doi:10.5194/bg-13-3051-2016, 2016.
- Hommeltenberg, J., Mauder, M., Drösler, M., Heidbach, K., Werle, P. and Schmid, H. P.: Ecosystem scale methane fluxes in a natural temperate bog-pine forest in southern Germany, *Agric. For. Meteorol.*, 198, 273–284, doi:10.1016/j.agrformet.2014.08.017, 2014.
- Hurkuck, M., Brümmer, C. and Kutsch, W. L.: Near-neutral carbon dioxide balance at a seminatural, temperate bog ecosystem, *J. Geophys. Res. G Biogeosciences*, 121(2), 370–384, doi:10.1002/2015JG003195, 2016.
- Krinner, G., Viovy, N., de Noblet-Ducoudré N., Ogée, J., Polcher, J., Friedlingstein, P., Ciais, P., Sitch, S. and Prentice, I. C.: A dynamic global vegetation model for studies of the coupled atmosphere-biosphere system, *Global Biogeochem. Cycles*, 19(1), 1–33, doi:10.1029/2003GB002199, 2005.
- Lafleur, P. M., Moore, T. R., Roulet, N. T. and Frohling, S.: Ecosystem respiration in a cool

- temperate bog depends on peat temperature but not water table, *Ecosystems*, 8(6), 619–629, doi:10.1007/s10021-003-0131-2, 2005.
- Laggoun-Défarge, F., Gogo, S., Bernard-Jannin, L., Guimbaud, C., Zoccatelli, R., Rousseau, J., Binet, S., D'Angelo, B., Leroy, F., Jozja, N., Le Moing, F., and , Défarge , C.: DOES HYDROLOGICAL RESTORATION AFFECT GREENHOUSE GASES EMISSION AND PLANT DYNAMICS IN SPHAGNUM PEATLANDS ?, *Mires. Peat.*, 2016.
- Lund, M., Lindroth, A., Christensen, T. R. and Ström, L.: Annual CO<sub>2</sub> balance of a temperate bog, *Tellus B*, 59(5), 804–811, 2007.
- Lund, M., Christensen, T. R., Lindroth, A. and Schubert, P.: Effects of drought conditions on the carbon dioxide dynamics in a temperate peatland, *Environ. Res. Lett.*, 7(4), 45704, 2012.
- Lund, M., Bjerke, J. W., Drake, B. G., Engelsen, O., Hansen, G. H., Parmentier, F.-J. W., Powell, T. L., Silvennoinen, H., Sottocornola, M., Tømmervik, H., Weldon, S. and Rasse, D. P.: Low impact of dry conditions on the CO<sub>2</sub> exchange of a Northern-Norwegian blanket bog, *Environ. Res. Lett.*, 10(2), 25004, doi:10.1088/1748-9326/10/2/025004, 2015.
- Malmer, N., Johansson, T., Olsrud, M. and Christensen, T. R.: Vegetation, climatic changes and net carbon sequestration in a North-Scandinavian subarctic mire over 30 years, *Glob. Chang. Biol.*, 11(11), 1895–1909, doi:10.1111/j.1365-2486.2005.01042.x, 2005.
- McVeigh, P., Sottocornola, M., Foley, N., Leahy, P. and Kiely, G.: Meteorological and functional response partitioning to explain interannual variability of CO<sub>2</sub> exchange at an Irish Atlantic blanket bog, *Agric. For. Meteorol.*, 194, 8–19, doi:10.1016/j.agrformet.2014.01.017, 2014.
- Merbold, L., Kutsch, W. L., Corradi, C., Kolle, O., Rebmann, C., Stoy, P. C., Zimov, S. A. and SCHULZE, E.: Artificial drainage and associated carbon fluxes (CO<sub>2</sub>/CH<sub>4</sub>) in a tundra ecosystem, *Glob. Chang. Biol.*, 15(11), 2599–2614, 2009.
- Milecka, K., Kowalewski, G., Fiałkiewicz-Kozieł, B., Gałka, M., Lamentowicz, M., Chojnicki, B. H., Goslar, T. and Barabach, J.: Hydrological changes in the Rzecin peatland (Puszcza Notecka, Poland) induced by anthropogenic factors: Implications for mire development and carbon sequestration, *The Holocene*, 959683616670468, 2016.
- Nilsson, M., Sagerfors, J., Buffam, I., Laudon, H., Eriksson, T., Grelle, A., Klemetsson, L.,

- Weslien, P. E. R. and Lindroth, A.: Contemporary carbon accumulation in a boreal oligotrophic minerogenic mire—A significant sink after accounting for all C-fluxes, *Glob. Chang. Biol.*, 14(10), 2317–2332, 2008.
- Olefelt, D., Roulet, N. T., Bergeron, O., Crill, P., Bäckstrand, K. and Christensen, T. R.: Net carbon accumulation of a high-latitude permafrost palsa mire similar to permafrost-free peatlands, *Geophys. Res. Lett.*, 39(3), doi:10.1029/2011GL050355, 2012.
- Pirk, N., Sievers, J., Mertes, J., Parmentier, F.-J. W., Mastepanov, M. and Christensen, T. R.: Spatial variability of CO<sub>2</sub> uptake in polygonal tundra - large overestimations by the conventional eddy covariance method, *Biogeosciences Discuss.*, 2016, 1–18, doi:10.5194/bg-2016-537, 2016.
- Reichstein, M., Falge, E., Baldocchi, D., Papale, D., Aubinet, M., Berbigier, P., Bernhofer, C., Buchmann, N., Gilmanov, T. and Granier, A.: On the separation of net ecosystem exchange into assimilation and ecosystem respiration: review and improved algorithm, *Glob. Chang. Biol.*, 11(9), 1424–1439, 2005.
- Riutta, T., Laine, J., Aurela, M., Rinne, J., Vesala, T., Laurila, T., Haapanala, S., Pihlatie, M. and TUITTILA, E.: Spatial variation in plant community functions regulates carbon gas dynamics in a boreal fen ecosystem, *Tellus B*, 59(5), 838–852, 2007.
- Sagerfors, J., Lindroth, A., Grelle, A., Klemedtsson, L., Weslien, P. and Nilsson, M. B.: Annual CO<sub>2</sub> exchange between a nutrient-poor, minerotrophic, boreal mire and the atmosphere, *J. Geophys. Res. Biogeosciences*, 113(1), 1–15, doi:10.1029/2006JDG000306, 2008.
- Sottocornola, M., Laine, A., Kiely, G., Byrne, K. A. and Tuittila, E. S.: Vegetation and environmental variation in an Atlantic blanket bog in South-western Ireland, *Plant Ecol.*, 203(1), 69–81, doi:10.1007/s11258-008-9510-2, 2009.
- Stiegler, C., Lund, M., Røjle Christensen, T., Mastepanov, M. and Lindroth, A.: Two years with extreme and little snowfall: Effects on energy partitioning and surface energy exchange in a high-Arctic tundra ecosystem, *Cryosphere*, 10(4), 1395–1413, doi:10.5194/tc-10-1395-2016, 2016.
- Sulman, B. N., Desai, A. R., Cook, B. D., Saliendra, N. and Mackay, D. S.: Contrasting carbon



dioxide fluxes between a drying shrub wetland in Northern Wisconsin, USA, and nearby forests, *Biogeosciences*, 6(6), 1115–1126, doi:10.5194/bg-6-1115-2009, 2009.

Vanselow-Algan, M., Schmidt, S. R., Greven, M., Fiencke, C., Kutzbach, L. and Pfeiffer, E. M.: High methane emissions dominated annual greenhouse gas balances 30 years after bog rewetting, *Biogeosciences*, 12(14), 4361–4371, doi:10.5194/bg-12-4361-2015, 2015.

Westergaard-Nielsen, A., Lund, M., Hansen, B. U. and Tamstorf, M. P.: Camera derived vegetation greenness index as proxy for gross primary production in a low Arctic wetland area, *ISPRS J. Photogramm. Remote Sens.*, 86, 89–99, doi:10.1016/j.isprsjprs.2013.09.006, 2013.

Zona, D., Oechel, W. C., Kochendorfer, J., Paw U, K. T., Salyuk, A. N., Olivas, P. C., Oberbauer, S. F. and Lipson, D. A.: Methane fluxes during the initiation of a large-scale water table manipulation experiment in the Alaskan Arctic tundra, *Global Biogeochem. Cycles*, 23(2), doi:10.1029/2009GB003487, 2009.